Surface & Coatings Technology 206 (2012) 4585–4593

Contents lists available at SciVerse ScienceDirect

Surface & Coatings Technology

journal homepage: www.elsevier.com/locate/surfcoat

Characteristics and tribological performance of DLC and Si-DLC films deposited on nitrile rubber

M. Lubwama [a,*], K.A. McDonnell [b], J.B. Kirabira [d], A. Sebbit [d], K. Sayers [c], D. Dowling [b], B. Corcoran [a]

[a] School of Mechanical and Manufacturing Engineering, Dublin City University, Dublin 9, Ireland
[b] School of Mechanical and Materials Engineering, University College Dublin, Dublin 4, Ireland
[c] Department of Mechanical Engineering, Dundalk Institute of Technology, Dundalk, Ireland
[d] Department of Mechanical Engineering, Makerere University, P.O. Box 7062, Kampala, Uganda

ARTICLE INFO

Article history:
Received 5 March 2012
Accepted in revised form 5 May 2012
Available online 12 May 2012

Keywords:
Coefficient of friction
Contact angle
Diamond-like carbon
Si-DLC film
Raman spectroscopy
Tribology

ABSTRACT

The characteristics and tribological performance of DLC and Si-DLC films with and without Si–C interlayers were studied in this paper. The films were deposited on nitrile rubber using a closed field unbalanced magnetron sputtering ion plating system. The film properties and characteristics were determined by scanning electron microscopy (SEM), hydrophobicity studies, Raman spectroscopy and tribological investigations. Tribological performance of these films was investigated using a pin-on-disc tribometer under applied loads of 1 N and 5 N under conditions of dry and wet sliding. The effect of immersing the films in water on tribological performance was also examined. The results show that the morphology of the films had a crack-like network. At a substrate bias of −30 V, the coatings were characterised by a very dense non-columnar microstructure. The highest value of the ratio of intensities of the D and G peaks (I_D/I_G) was 1.2 for Si-DLC film with Si–C interlayer. The lowest value of 0.7 was observed for DLC film. The contact angle (CA) of water droplets showed that the films were hydrophobic. These results are interpreted in terms of hybridisation of carbon in these coatings. The tribological investigation showed a dependence on both the tribological condition under investigation and the atomic percentage of Si in the films. At 5 N normal load the lowest wear depth was observed for DLC films.

1. Introduction

Diamond-like carbon (DLC) has been studied extensively for over four decades beginning with the work of Aisenberg and Chabot [1]. Carbon forms a great variety of crystalline and disordered structures because it is able to exist in three hybridisations; in the sp^3 configuration as in diamond, in the sp^2 configuration as in graphite and in the sp^1 configuration [2]. These unique characteristics have rendered DLC as an optimal solution for use as a protective coating due to a combination of relative high hardness, chemical inertness, and low friction coefficient and wear rates [3]. Doped or alloyed DLC coatings are an important category of DLC characterised by the incorporation of different elements into their structure. The addition of selected dopants is known to improve tribological properties of DLC [4].

More recently, the application of DLC coatings onto rubber substrates has received significant attention in the literature. Initial work of the application of DLC coatings on polymer substrates appeared briefly through the work of Ollivier et al. [5], who assessed the adhesion of DLC on polyethylene terephthalate (PET). However, it was not until the work of Nakahigashi et al. [6] that the structural, mechanical and tribological properties of DLC coatings applied to various rubber substrates were discussed more explicitly. More recently, Martinez et al. [7] has applied DLC coatings to elastomer frictional surfaces using plasma enhanced chemical vapour deposition (PECVD) process and investigated the hydrophobicity, surface analysis and tribology of these films applied on various nitrile rubbers (NBR). The de Hosson group [8–10] have applied DLC on various rubber substrates including hydrogenated nitrile rubber (HNBR) and acrylic rubber (ACM) using a combination of PECVD and closed field unbalanced magnetron sputtering processes. They and other researchers [11–13] have determined the tribological performance of DLC coatings on rubber substrates, hence, enhancing our current understanding of DLC coatings on rubber substrates.

Previous studies on the tribological performance of DLC coatings on rubber substrates have shown an improvement in the tribological performance under dry sliding [6–10,14]. Very few studies have investigated sliding in an aqueous environment. Studies concerning DLC coatings in water sliding [15], and the relationships of DLC coatings to humidity [16,17], were based on coatings applied to either silicon (Si) wafers or various metallic substrates, and not onto rubber substrates. One aspect of coating performance that has been neglected is the performance of DLC coated on rubber under dry and wet sliding tribo-tests and after immersion in water.

* Corresponding author. Tel.: +353 85 229 5129; fax: +353 1 700 5345.
E-mail address: michael.lubwama2@mail.dcu.ie (M. Lubwama).

0257-8972/$ – see front matter © 2012 Elsevier B.V. All rights reserved.
doi:10.1016/j.surfcoat.2012.05.015

Table 1
Elemental composition of coatings applied to NBR by energy dispersive X-ray spectroscopy. The composition is compared to compositional results for DLC on NBR 7201, NBR 9003 and NBR 8002 from the work of Martinez et al. [7].

	C (at.%)	O (at.%)	Si (at.%)	N (at.%)	Other (at.%)
DLC	87.7	12.2	0.1	–	Trace
Si-DLC	85.6	11.4	2.9	–	Trace
DLC with Si–C interlayer	87.2	7.3	5.5	–	Trace
Si-DLC with Si–C interlayer	85.3	10.5	4.0	–	0.2
DLC on NBR 7201	87.7	7.9	1.6	2.7	Trace
DLC on NBR 9003	88.6	7.9	1.3	1.3	Trace
DLC on NBR 8002	98.3	1.3	0.3	–	–

Si incorporation has been widely studied and is reported as being effective in reducing friction coefficients in ambient humid air with only limited deterioration of the wear resistance [18]. This has been attributed to the formation of SiO_2 wear particles and their interaction with the humid environment through tribo-chemical effects [19]. Gradient a-SiC_x interlayers were reported to improve adhesion after evaluation by scratch tests [20]. The improved adhesion was due to the fact that SiC is chemically more compatible to oxides due to the stability of SiO_x and their mixture with SiC materials.

A potential application for such coatings is to enhance the performance of nitrile rubber piston seals in handpumps for rural water supply in developing countries by reducing their wear rates. Such seals experience a combination of dry and wet sliding and prolonged aqueous immersion depending on the height of the local water table and operating regime. Functioning handpumps are in short supply. As a consequence the duty cycle for pump seals is heavy. This study therefore aims to examine potential remedies that DLC and Si-DLC films with or without Si–C interlayers applied to nitrile rubber substrates may offer.

2. Experimental details

High quality black acrylonitrile butadiene rubber (NBR) of 3 mm thickness was used as substrate material in this work. Hydrogenated DLC (a-C:H) films were deposited on NBR by closed field unbalanced magnetron sputter ion plating (CFUBMSIP) system in a Teer UDP/450 sputtering rig. A pulsed d.c. (p-DC) power unit (Advanced Energy) was used as substrate bias source, operating at a frequency of 150 kHz with a pulse off time of 150 ns at a substrate voltage bias of −30 V. This bias voltage was maintained during the entire deposition process. Three pieces of NBR rubber 100 mm by 100 mm by 3 mm were coated in each batch. Two opposite magnetrons were used as carbon targets and one magnetron was used as the Si target. The fourth magnetron in the system was not used during the deposition process. The samples were mounted on a holder in the centre of the system facing outwards towards the target. The sample rotation speed was 5 rpm. A sputter cleaning process was integrated into the deposition process so as to avoid re-contamination between the cleaning and deposition process [21]. The NBR substrates were etched in Ar plasma for 10 min at a bias of 200 V in order to clean the surface of contaminants and improve the adhesion of the carbonaceous layer. The total deposition time for DLC was 60 min. This process was repeated for all samples including the Si-DLC samples. Ar and C_4H_{10} gases were fed into the chamber via mass flow controllers. The gas flow rates ($Ar/C_4H_{10} = 12$ sccm/8 sccm) were kept constant during the deposition. In order to achieve the dopant of Si in Si-DLC, a current of 0.5 A was supplied to the Si target during the deposition. The Si–C interlayer was obtained by supplying a current of 1 A to the Si target and 1 A to the pure C target. The Si–C interlayer deposition time was 35 min and the subsequent time for DLC deposition was 40 min. Table 1 shows the elemental surface composition for the coatings obtained by energy dispersive X-ray spectroscopy.

The tribological performance was evaluated at room temperature using a pin-on-disc (POD 2) tribometer. The counterpart was a standard Ø5 mm commercial WC–Co ball. WC–Co ball was used as counterpart material because it has a higher Vickers hardness value [22,23], compared to the typical 100Cr6 steel balls used [24]. Two different tests were performed on each sample at a linear sliding speed of 10 cm/s at correlative test track diameters of 6 and 10 mm. Three repetitions at 5000 revolutions were carried out for each film. In addition, two different loads have been studied, 1 N and 5 N. Wet sliding

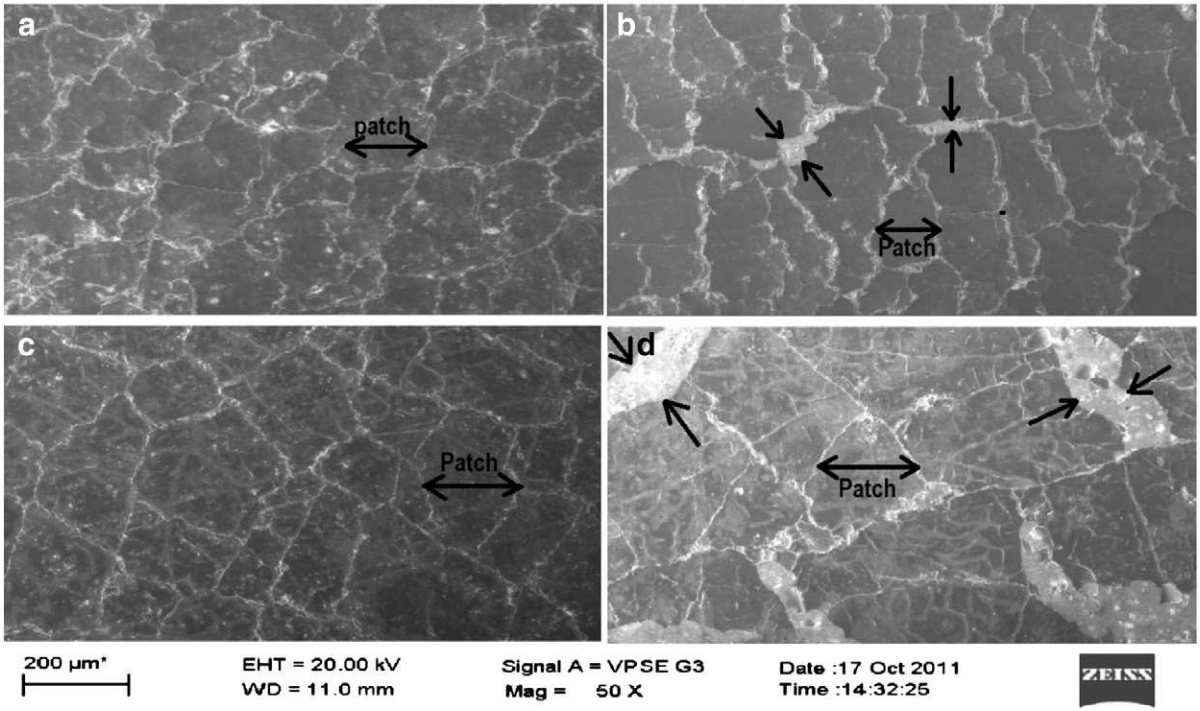

Fig. 1. Overview of the surface morphology for: a — DLC; b — Si-DLC; c — DLC with Si–C interlayer; d — Si-DLC with Si–C interlayer. Two arrows indicate partially delaminated bands in b and c.

conditions were achieved by attaching a pipette filled with water adjacent to the pin such that its position ensured that the continuous flow of water was dispensed. Prior to commencement of wet sliding tests, water was dispensed onto the coated samples so that an initial boundary lubrication contact was achieved. Tribo-tests at 1 N and 5 N were also carried out on the coated samples after these samples were immersed in water for four days.

The microstructure was characterised by scanning electron microscopy (SEM), using an EVO LS 15 SEM operating at 20 kV acceleration voltage under variable pressure mode. The surface roughness of the coatings was determined by a Dektak 150 surface profiler with a low-inertia sensor (LIS). A stylus force of 1 mg over a scanning range of 2 mm was used for the surface roughness measurements. The thickness of DLC and Si-DLC coatings on NBR was estimated by measuring the step height of DLC coating on a Si wafer which was deposited using the same process conditions.

The coating thickness for DLC and Si-DLC films deposited on NBR with Si–C interlayers was estimated using a SEM after immersion in liquid nitrogen for 10 min and fracturing. Raman spectra were acquired to investigate the chemical bonding of these films by using a LabRAM Horiba Jobin Yvon spectrometer equipped with a CCD detector and an Ar laser (488 nm) at 8 mW. All of the measurements were recorded for the wavelength range of 500 to 2000 cm^{-1} using the same conditions (5 s of integration time and 5 accumulations) with a 100× magnification objective and a 200 μm pinhole.

Static contact angle (CA) measurements were carried out using a DataPhysics OCA 20 machine at room temperature by the Sessile Drop Method using liquid droplets of 1 μl [7]. The CA measurements were repeated at least six times on each sample in order to minimise the measurement uncertainty. The liquids used as reference liquids for the surface free energy calculation were water, ethylene glycol and diiodomethane [7]. The surface free energy was calculated by the Owens–Wendt–Rabel and Keable method that was recommended for coatings applied to polymer substrates from which the dispersive and polar components of the polar energy were easily determined [25].

3. Results and discussion

3.1. Surface morphology

An overview of the surface morphology of the DLC and Si-DLC films coated on NBR is shown in Fig. 1a and b. The evolution of the

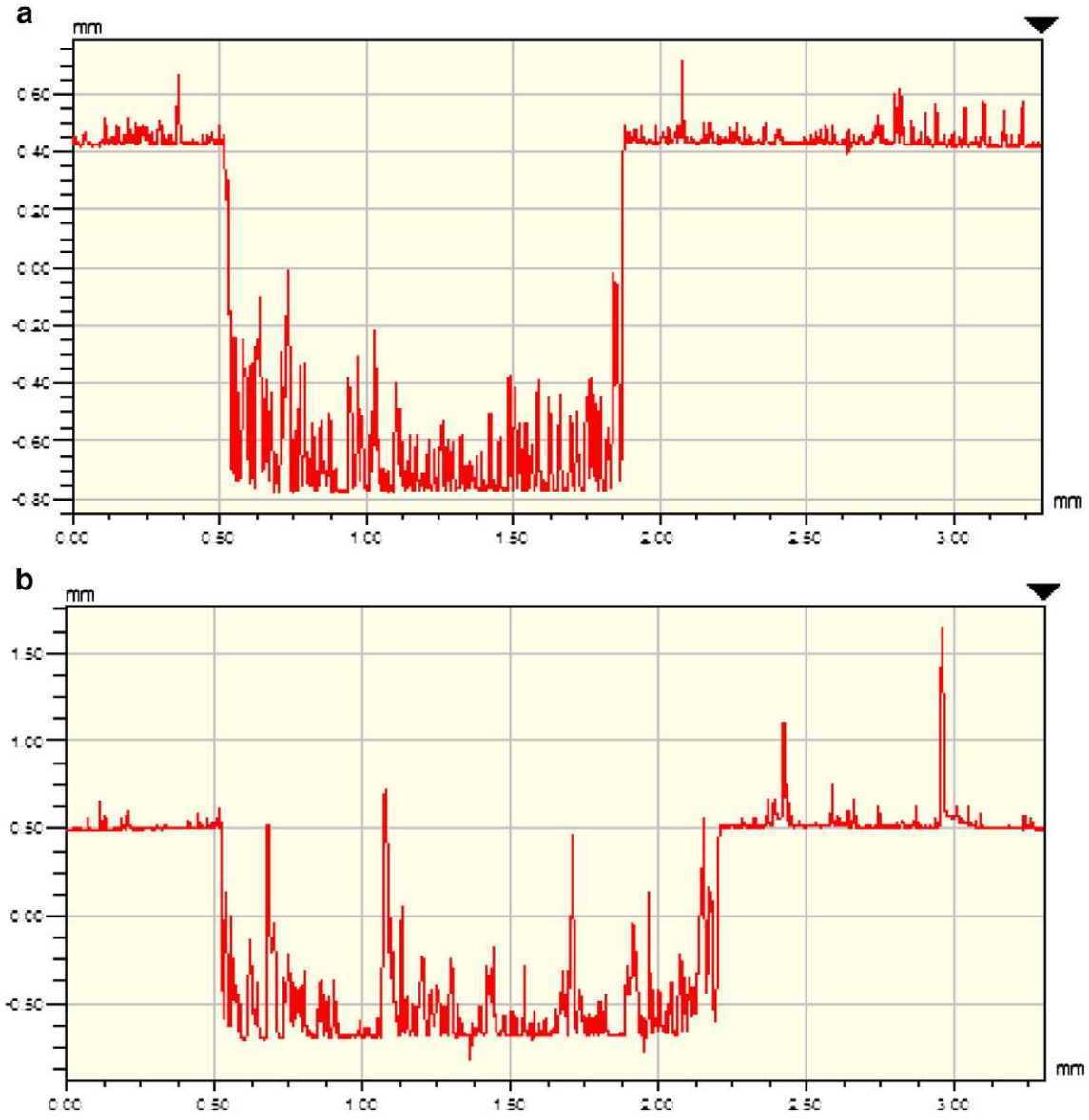

Fig. 2. Step profile of the surface topography tracing after unmasking the coating for DLC (a) and Si-DLC coatings on Si wafer substrates.

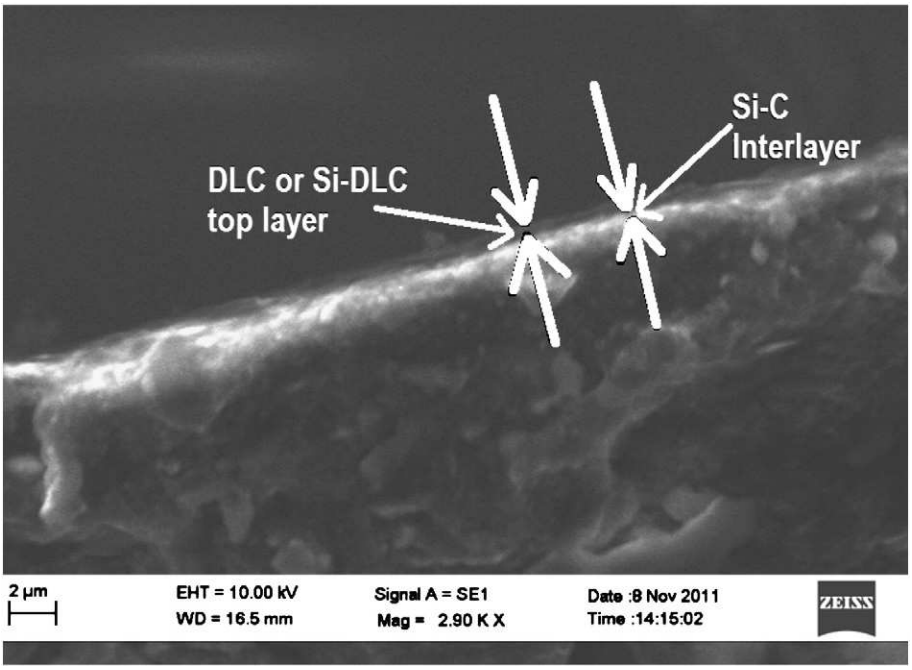

Fig. 3. SEM micrograph of the fracture cross-section of DLC and/or Si-DLC with Si–C interlayers.

microstructure as a result of the inclusion of the Si–C interlayer is also shown in Fig. 1c, and d. The surface morphology of DLC deposited on rubber substrates is characterised by a dendritic crack-like network [7,26]. These cracks originate at the first atomic layer of DLC on rubber due to thermal stress mismatch and continuously grow upwards together with the film itself resulting in a patch size of the DLC films in the micrometre scale range [27]. The presence of a dendritic micro-crack like network has been recognised as contributing positively to the performance of the DLC coatings on rubber due to the improvement in flexibility of the coating when the substrate deforms without interfacial delamination [14]. However, from Fig. 1b and d, which shows the surface morphology of Si-DLC coating without Si–C interlayer and Si-DLC coating with Si–C interlayer, more areas for potential delamination were observed. This may be attributed to the effect of Si dopant in the film, which causes an increase in contributions from sp^3 sites due to vibration in C – C sp^3 bonds [28]. Also, in the Si-DLC higher values of the full width half maximum (FWHM) of the Si-DLC films were observed. From Raman studies discussed later on, the higher values of FWHM indicate that the graphitic clusters were more strained in this case [29]. Fig. 2 shows the coating thickness for both DLC and Si-DLC coatings deposited on Si wafer substrates. The thickness of these coatings was approximately 1.2 µm. The coating thickness determined by this approach produced similar results to coating thickness on rubber with the minor differences observed being within the error of observation due to the rough interface of rubber substrates [30]. Fig. 3 shows the coating thickness after fracturing of DLC and/or Si-DLC with Si–C interlayer. The coating thickness estimated by using scanning electron microscopy was

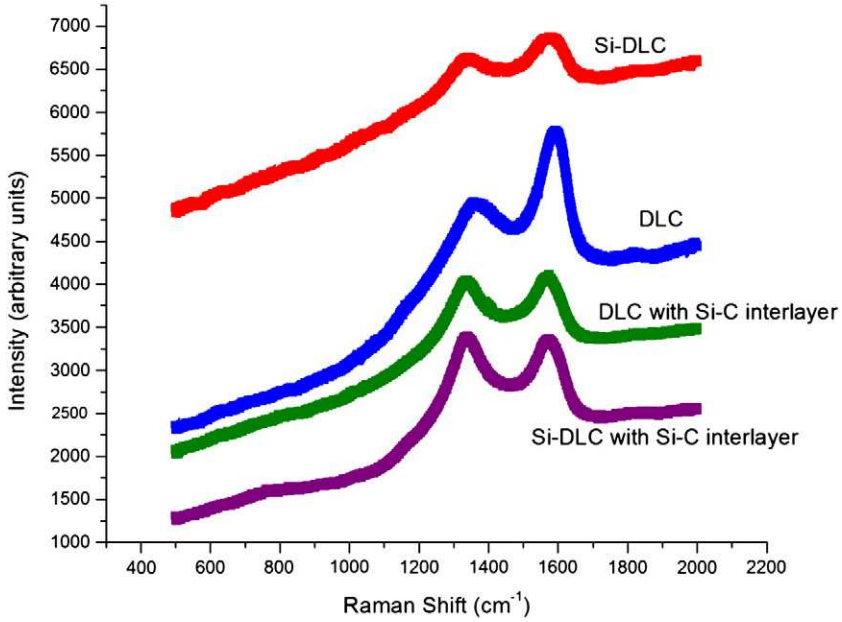

Fig. 4. Raman spectra of DLC and Si-DLC films.

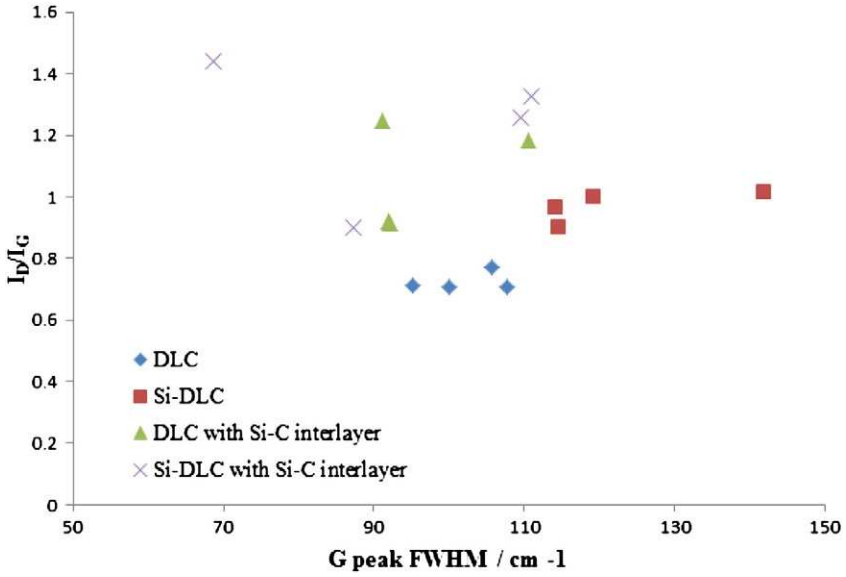

Fig. 5. The ratio of the intensities of the D peak, I_D, and G peak, I_G, plotted against the fitted FWHM.

approximately 500 nm for Si–C interlayer and approximately 500 nm for the top DLC or Si-DLC film.

The fracture cross-section did not show the typical columnar structure for DLC coatings deposited on rubber. Bui et al. showed that for DLC coatings on Si wafer, a bias voltage of 100 V was enough to prevent column formation leading to a dense, columnar free and featureless structure. The deposition method they used was an unbalanced reactive magnetron sputtering with a closed field system [30]. Columnar growth has been related to interface structure of the growing coating, which is controlled by the intensity of concurrent ion impingement [31]. In this study, a closed field unbalanced magnetron sputtering ion plating system was used where the coating deposition is carried out using a high density of low energy bombarding ions (−30 V bias voltage in this case), resulting in very dense, non-columnar coating structures. The bias voltage is even lower than the bias voltage of −50 V (in magnitude terms) described in the paper by Bui et al. who investigated the influence of different voltage biases on the surface morphology [30]. In this configuration, the plasma that is present between the source and the NBR substrate is ideal for ion plating since the plasma is present to allow energetic ions to bombard the substrate and enhance ionisation of the vapour species at low energies [32].

3.2. Raman spectroscopy

Fig. 4 represents typical full spectra for samples of DLC and Si-DLC coatings, showing the prominent G peak (centred at approximately 1580 cm^{-1}) and a smaller underlying D peak (centred at approximately 1350 cm^{-1}). The individual G and D peaks from the spectra were fitted with Gaussian line shapes to quantify their respective full width half maximum (FWHM) and peak heights. Such an approach was used by Tamor et al. [33]. Also, presence of the D peak in most of the spectra from these DLC and Si-DLC films prohibited the use of a single Breit–Wigner–Fano (BWF) line shape to quantify the sp^2:sp^3 ratio [34]. The G peak is mainly sensitive to the configuration of sp^2 sites because of their higher cross-section. Thus, the ratio of the intensities of the D peak, I_D, and G peak, I_G, I_D/I_G, would be a measure of the sp^2 phase organised in rings [29]. Therefore, I_D/I_G can be used as a parameter for qualitatively evaluating the sp^3 bond content [35]. The FWHM of the G-peak is mainly sensitive to structural disorder, which arises from bond angle and bond length distortions. The FWHM of the G-peak would be small if the clusters were defect free, unstrained or molecular [29]. A plot of the ratio of the intensities of the D peak, I_D, and G peak, I_G, to the fitted peak width is shown in Fig. 5. The data points are more clustered for DLC and Si-DLC, than they are for DLC and Si-DLC with Si–C interlayer. A plot of I_D/I_G vs. G peak width should give a straight line as the G peak width is partially determined by the graphitic cluster size [36]. However, Filik et al. [34] observed that a linear relationship between G peak width and the I_D/I_G held for films deposited at DC bias values greater than approximately 150 V, while, for films deposited at DC bias values lower than 150 V, data points were more clustered, similar to the results shown in Fig. 5. The clustering of the DLC and Si-DLC films might be due to the presence of H-terminated aromatic groups, rather than extended networks of graphene sheets, which suggests that at these lower ion impact energies the graphitic clusters have much less influence upon the G-peak width [34]. The ratio of the intensities of the D and G bands (I_D/I_G) generally tended to increase in both the DLC film compared to DLC with Si–C interlayer and for the Si-DLC film compared to Si-DLC with Si–C interlayer, which indicates that the sp^2 content is increasing. Average values of I_D/I_G showed DLC film with an intensity ratio of approximately 0.7 and DLC film with a

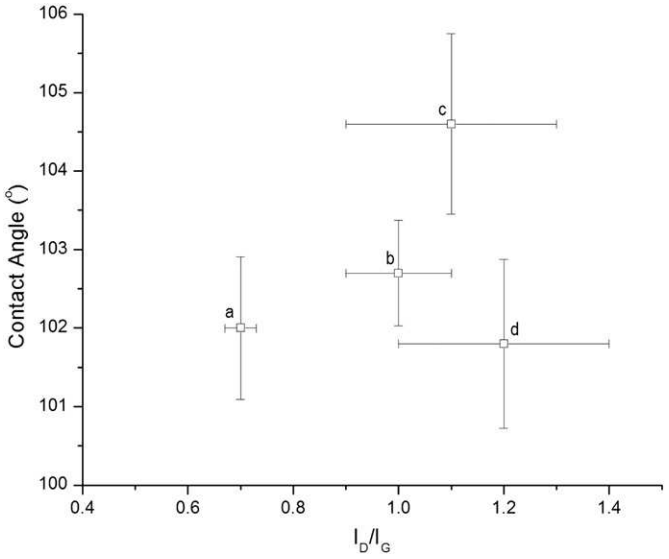

Fig. 6. Relation between contact angle and intensity ratio for DLC — a, Si-DLC — b; DLC with Si–C interlayer — c; and Si-DLC with Si–C interlayer — d.

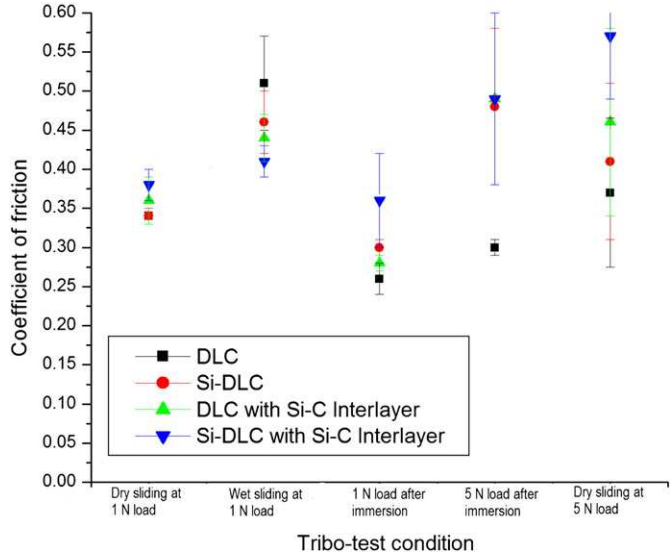

Fig. 8. Average friction coefficient of DLC and Si-DLC coatings under different tribo-testing conditions.

the Si–C in the DLC coatings resulted in an increase in CA for DLC film with Si–C interlayer when compared to DLC film.

The increase in the roughness of hydrophobic surfaces has been reported as being responsible for drastic decreases of water contact angle [7]. As shown in Fig. 1, the surface pattern of the coatings is characterised by a network of micro-cracks, with varying patch sizes. Fig. 7 shows the surface profile for DLC coatings on the NBR substrate. The average surface roughness for DLC coatings and Si-DLC coatings, with and without the inclusion of the Si–C interlayer was equivalent with measured values ranging from 1.5 μm to 2.2 μm. These results indicated an increase in the surface roughness of the coatings when compared to an uncoated substrate which had a measured average roughness of about 1 μm. An increment in surface roughness was also observed in the study by Martinez et al. [7]. However, since the inclusion of the Si–C interlayer did not have a significant contribution on surface roughness minimal effects on the contact angle measurements as a result of the surface roughness should be expected [7].

Table 2 shows the surface free energy (mJ/m^2) of the studied samples determined by the Owens–Wendt–Rabel and Keable method. The inclusion of the Si–C interlayer increases the surface free energy of the films. A higher surface free energy is observed for Si-DLC with the Si–C interlayer (with lower water CA) compared to a lower surface energy for DLC with Si–C interlayer (with higher water CA). The inclusion of the Si–C interlayer suppressed the polar component of the surface free energy. This is contrary to the observations by Martinez et al. [7]. The higher atomic percentages of silicon and lower atomic percentages of oxygen observed for films with Si–C interlayers in Table 1 may be responsible for this result.

3.4. Tribological performance

The results on the frictional behaviour are shown in Figs. 8 and 9. In the work by Nakahigashi et al. [6], the average coefficient of friction for DLC coating on NBR was 0.6 for a normal load of 0.1 N. In this paper the average coefficients of friction were lower than the value reported by Nakahigashi et al. From Fig. 8, the average coefficients of friction for the DLC and Si-DLC film with and without Si–C interlayers was approximately 0.34 for applied load of 1 N under dry sliding. However, under the condition of wet sliding at 1 N load, the highest coefficient of friction was observed for DLC coating at 0.51 ± 0.06 (mean ± standard deviation). The lower coefficients of friction are found for the films that had highest Si (at.%) incorporation. An increase in Si content in DLC could reduce the coefficient of friction due to acceleration of tribo-chemical reactions with water to form hydroxyl groups ($SiO_x(OH)_y$) [15]. All of the samples show a friction increase between 0.25 and 0.4 at 200 to 400 revolutions to between 0.45 and 0.6 at 4000 to 5000 revolutions indicating a clear transition region as shown in Fig. 9. The frictional behaviour from initial friction

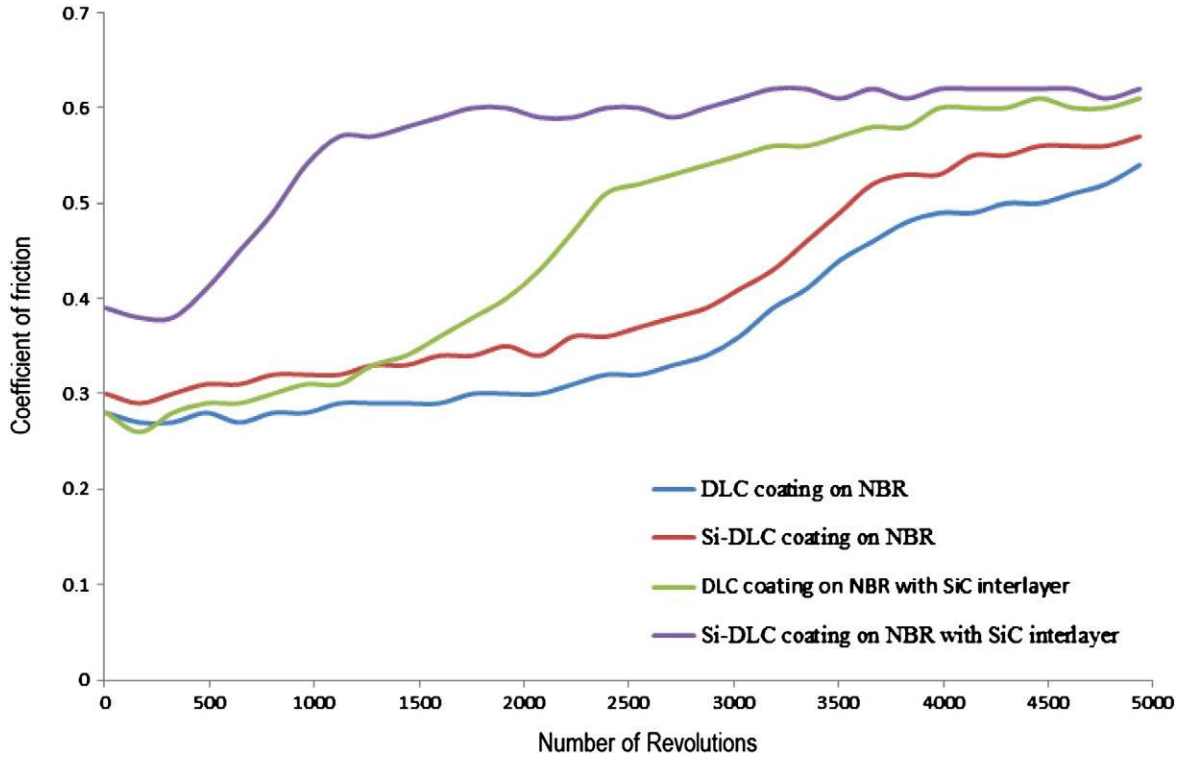

Fig. 9. Frictional behaviour for DLC and Si-DLC films for dry sliding under applied load of 5 N.

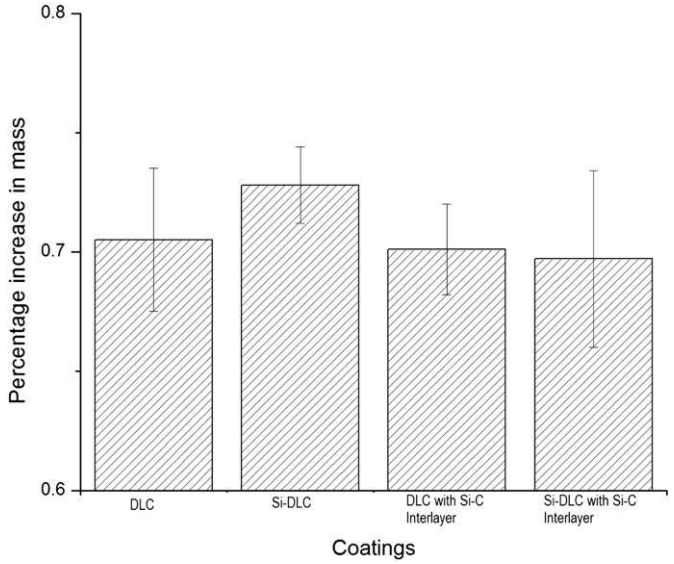

Fig. 10. Percentage increase in mass of the various coating categories after immersion in water.

and the friction performance vs. number of revolutions may be explained by the differences in composite micro-hardness between the coatings as a result of the inclusion of the Si–C interlayer. From Fig. 10, it was observed that there was no significant variation in the percentage increase in mass between the coatings after immersion in water for four days; however, lower coefficient of friction was observed for all of the coatings tested at normal load of 1 N after immersing in water for four days. This may be a result of low surface energy due to water absorption which passivises rapidly the dangling bonds on the wear scars, much in the same way as an increase in relative humidity reduces wear rate [17]. The performance under a load of 5 N was expected to indicate a higher coefficient of friction. The performance of the DLC coating under this testing condition showed a lower coefficient of friction than the Si-DLC film and the DLC and Si-DLC films with Si–C interlayers. This result indicates that at higher loads there may be a detrimental effect due to the inclusion of Si. A similar observation can be made for tests carried out under dry sliding for normal load of 5 N. This may be explained by a decrease in the hardness and modulus of the coatings as a result of doping with Si, even in very small amounts [39].

Table 3
Average wear depth (mm) of the study samples under testing condition of load 5 N for dry sliding and after immersion in water for 4 days.

Sample	Dry sliding at load of 5 N	Dry sliding at load of 5 N after immersing in water
DLC	0.068	0.008
Si-DLC	0.073	0.130
DLC with Si–C interlayer	0.100	0.163
Si-DLC with Si–C interlayer	0.123	0.115

At low load (1 N) the surfaces of the films were almost unmodified making it difficult to obtain even qualitative information of the wear through characterisation techniques such as SEM. Fig. 11 shows the wear profile of the wear tracks formed on the films obtained after tribo-testing for dry sliding under a load of 5 N, which indicate non-uniformity of the wear track. The wear depth for each film was calculated by taking the average of two depths, W_1, and W_2, associated with the maximum locations below the datum line (0.00) for each trace along the diameter from the outermost circumference of the wear track. The non-uniformity of the wear track can be explained

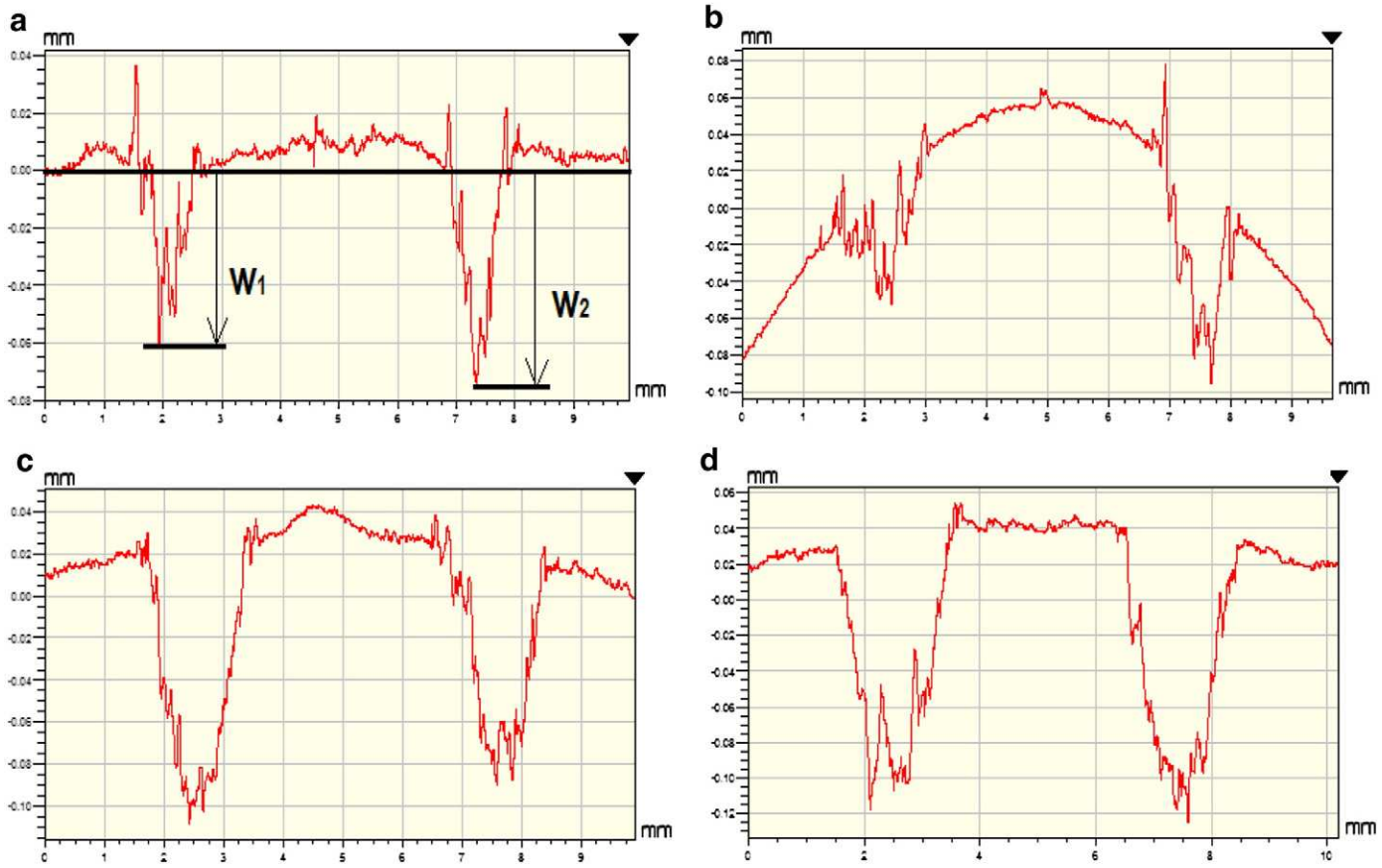

Fig. 11. Wear profile of the wear tracks for the films under dry sliding for load of 5 N. DLC — a; Si-DLC — b; DLC with Si–C interlayer — c; Si-DLC with Si–C interlayer — d.

by the high deformation and elasticity of the rubber substrate. Table 3 shows the average wear depth for the films after testing at normal load of 5 N under dry sliding and after immersing in water. The results of the wear depth show less material loss for the DLC films. These results correlate well with the results for the frictional characteristics of the films. However, in comparison to coating thickness wear depth is about three orders of magnitude larger for tribo-tests at normal load of 5 N. The DLC films that have the lowest material loss as measured by the lowest wear depth also had the lowest coefficient of friction for these conditions. From the Raman spectroscopy results it was determined that the inclusion of Si–C interlayer results in an increase in sp^2 clusters, as such DLC and Si-DLC films with Si–C interlayers may have lower micro-hardness, which explains their higher wear depth compared to DLC and Si-DLC without Si–C interlayer. Doping with Si results in a decrease in hardness [39]. This explains the higher wear depth for Si-DLC compared to DLC and may also explain the distinct curvature for Si-DLC in Fig. 11b.

4. Conclusion

DLC and Si-DLC films with and without Si–C interlayers were deposited on a NBR using a closed field unbalanced magnetron sputtering ion plating system. The characteristic crack-like microstructure typical for DLC coatings on rubber was observed for the coatings deposited in this study. At a substrate bias of −30 V, the coatings were characterised by a very dense non-columnar microstructure. The highest value of the ratio of intensities of the D and G peaks (I_D/I_G) was 1.2 for Si-DLC film with Si–C interlayer. The lowest value of 0.7 was observed for DLC film. The CA of water droplets showed that the films were hydrophobic. The tribological investigation showed a dependence on both the tribological condition under investigation and the atomic percentage of Si in the films. These results indicate that the potential of applying DLC and Si-DLC films with and without Si–C interlayers onto actual piston seals may present some advantages.

Acknowledgements

The authors would like to acknowledge the financial support provided by the Water is Life project under Irish Aid and Higher Education Authority partnership of the Republic of Ireland for the financial support to carry out the research.

References

[1] S. Aisenberg, R. Chabot, J. Appl. Phys. 42 (1971) 2953.
[2] J. Robertson, Adv. Phys. 35 (1986) 317.
[3] J. Robertson, Mater. Sci. Eng. R 37 (2002) 129.
[4] J.C. Sanchez, A. Fernandez, in: C. Donnet, A. Erdemir (Eds.), Springer Science and Business Media, LLC, New York, USA, 2008, p. 311.
[5] B. Ollivier, S.J. Dowey, S.J. Young, A. Matthews, J. Adhes. Sci. Technol. 9 (1995) 769.
[6] T. Nakahigashi, Y. Tanaka, K. Miyake, H. Oohora, Trib. Int. 37 (2004) 907.
[7] L. Martinez, R. Nevshupa, L. Alvarez, Y. Huttel, J. Mendez, E. Roman, E. Mozas, J.R. Valdes, M.A. Jimenez, Y. Gachon, C. Heau, F. Faverjon, Trib. Int. 42 (2009) 584.
[8] D. Martinez-Martinez, M. Schenkel, Y.T. Pei, J.Th.M. De Hosson, Thin Solid Films 519 (2011) 2213.
[9] D. Martinez-Martinez, M. Schenkel, Y.T. Pei, J.C. Sanchez-Lopez, J.Th.M. De Hosson, Surf. Coat. Technol. 205 (2011) S75.
[10] X.L. Bui, Y.T. Pei, E.D.G. Mulder, J.Th.M. De Hosson, Surf. Coat. Technol. 203 (2009) 1964.
[11] M. Ikeyama, H. Masuda, T. Miyajima, J. Choi, Surf. Coat. Technol. 206 (2011) 999.
[12] N. Miyakawa, S. Minamisawa, H. Takikawa, T. Sakakibara, Vaccine 73 (2004) 611.
[13] H. Takikawa, N. Miyakawa, S. Minamisawa, T. Sakakibara, Thin Solid Films 457 (2004) 143.
[14] Y.T. Pei, X.L. Bui, X.B. Zhou, J.Th.M. De Hosson, Surf. Coat. Technol. 202 (2008) 1869.
[15] X. Wu, M. Suzuki, T. Ohana, A. Tanaka, Diamond Relat. Mater. 17 (2008) 7.
[16] S.J. Park, J.K. Kim, K.R. Lee, D.H. Ko, Diamond Relat. Mater. 12 (2003) 1517.
[17] J. Jiang, S. Zhang, R.D. Arnell, Surf. Coat. Technol. 167 (2003) 221.
[18] R. Gilmore, R. Hauert, Thin Solid Films 398–311 (2001) 119.
[19] T. Michler, M. Grischke, K. Bewilongua, A. Hieke, Surf. Coat. Technol. 111 (1999) 41.
[20] B.H. Jung, M.J. Chiang, M.H. Hon, Mater. Chem. Phys. 72 (2001) 163.
[21] P.M. Martin, Handbook of Deposition Technologies for Films and Coatings, 2009, p. 23.
[22] U. Sen, S. Sen, F. Yilmaz, Ind. Lubr. Trib. 57 (2005) 243.
[23] S. Kurzenhauser, V. Hegadekatte, J. Scheider, N. Huber, O. Kraft, K.-H. Sum Gahr, Microsyst. Technol. 14 (2008) 1839.
[24] M. Sedlacek, B. Podgornik, J. Vizintin, Mater. Char. 59 (2008) 151.
[25] S. Okuji, H. Boldyreyeva, Y. Takeda, N. Kishimoto, Nucl. Instrum. Meth. B 267 (2009) 1557.
[26] M. Schenkel, D. Martinez-Martinez, Y.T. Pei, J.Th.M. De Hosson, Surf. Coat. Technol. 205 (2011) 4838.
[27] Y.T. Pei, X.L. Bui, J.Th.M. De Hosson, Thin Solid Films 518 (2010) S42.
[28] K.W.R. Gilkes, S. Prawer, K.W. Nugent, J. Robertson, H.S. Sands, Y. Lifshitz, X. Shi, J. Appl. Phys. 87 (2000) 7283.
[29] R. Paul, S.N. Das, S. Dalui, R.N. Gayen, R.K. Roy, R. Bhar, A.K. Pal, J. Phys. D Appl. Phys. 41 (2008) 055309.
[30] X.L. Bui, Y.T. Pei, J.Th.M. De Hosson, Surf. Coat. Technol. 202 (2008) 4939.
[31] Y.T. Pei, C.Q. Chen, K.P. Shaha, J.Th.M. De Hosson, J.W. Bradley, S.A. Voronin, M. Cada, Acta Mater. 56 (2008) 696.
[32] U. Helmersson, M. Lattemann, J. Bohlmark, A.P. Ehiasarian, J.T. Gudmundsson, Thin Solid Films 513 (2006) 1.
[33] M.A. Tamor, W.C. Vassell, J. Appl. Phys. 76 (1994) 3823.
[34] J. Filik, P.W. May, S.R.J. Pearce, R.K. Wild, K.R. Hallam, Diamond Relat. Mater. 12 (2003) 974.
[35] A.C. Ferrari, J. Robertson, Phys. Rev. B 61 (2000) 14095.
[36] J. Schwan, S. Ulrich, V. Batori, H. Errhardt, J. Appl. Phys. 80 (1996) 440.
[37] N. Paik, Surf. Coat. Technol. 200 (2005) 2170.
[38] C. Casiraghi, A.C. Ferrari, J. Robertson, Phys. Rev. B 72 (2005) 085401.
[39] P. Papakonstantinou, J.F. Zhao, P. Lemoine, E.T. McAdams, J.A. McLaughlin, Diamond Relat. Mater. 11 (2004) 1074.